Distance-Dependent Diffusion-Controlled Reaction of •NO and O2•− at Chemical Equilibrium with ONOO−

Horacio Botti,[*,†,‡] **Matías N. Möller,**[‡,§,∥] **Daniel Steinmann,**[#,⊥] **Thomas Nauser,**[#]
Willem H. Koppenol,[#] **Ana Denicola,**[‡,§] **and Rafael Radi**[*,‡,∇]

Unidad de Cristalografía de Proteínas, Instituto Pasteur de Montevideo, Montevideo, 11400, Uruguay, Center for Free Radical and Biomedical Research, Montevideo, 11800, Uruguay, Laboratorio de Fisicoquímica Biológica, Instituto de Química Biológica, Facultad de Ciencias, Universidad de la República, Montevideo, 11400, Uruguay, Department of Chemistry and Vanderbilt Institute of Chemical Biology, Vanderbilt University, Nashville, Tennessee 37240, United States, Institute of Inorganic Chemistry, Department of Chemistry and Applied Biosciences, ETH Zürich, CH-8093, Switzerland, and Departamento de Bioquímica, Facultad de Medicina, Universidad de la República, Montevideo, 11800, Uruguay

The fast reaction of •NO and O2•− to give ONOO− has been extensively studied at irreversible conditions, but the reasons for the wide variations in observed forward rate constants ($3.8 \leq k_f \leq 20 \times 10^9$ M^{-1} s^{-1}) remain unexplained. We characterized the diffusion-dependent aqueous (pH > 12) chemical equilibrium of the form •NO + O2•− = ONOO− with respect to its dependence on temperature, viscosity, and [ONOO−]$_{eq}$ by determining [ONOO−]$_{eq}$ and [•NO]$_{eq}$. The equilibrium forward reaction rate constant (k_f^{eq}) has negative activation energy, in contrast to that found under irreversible conditions. In contradiction to the law of mass action, we demonstrate that the equilibrium constant depends on ONOO− concentration. Therefore, a wide range of k_f^{eq} values could be derived ($7.5-21 \times 10^9$ M^{-1} s^{-1}). Of general interest, the variations in k_f can thus be explained by its dependence on the distance between ONOO− particles (sites of generation of •NO and O2•−).

I. Introduction

It is currently accepted that the main route to peroxynitrite anion [oxoperoxonitrate(1−), ONOO−] formation in biological systems is the spin-allowed, termination reaction between superoxide anion (O2•−) and nitric oxide (nitrogen monoxide, •NO), reaction 1A[1−3]

$$\text{•NO} + \text{O}_2^{\bullet -} \rightarrow \text{ONOO}^- \quad k_f \qquad (1A)$$

The first kinetic report supported a fast reaction between •NO and O2•−with a rate constant (k_f) on the order of 10^7 M^{-1} s^{-1}.[4] As a consequence of that report, the in vivo occurrence of peroxynitrite was proposed at that time and ONOOH was portrayed as a biologically relevant metal-independent source of the highly damaging HO•.[5−7] Currently, most authors agree that the reaction is diffusion limited.[3] Therefore, it is widely accepted that it will occur to some extent anytime these two radicals are available in the same compartment,[3,8] despite the facts that superoxide dismutases (SODs) compete with •NO for O2•− and that peroxynitrite has never been directly detected. Rate constants reported later that support this view were determined under irreversible conditions and are within a broad

range, 3.8×10^9 M^{-1} s$^{-1} \leq k_f^{irr} \leq 20.0 \times 10^9$ M^{-1} s^{-1}.[9−13] Nauser and co-workers proposed that the statistically significant discrepancy arises because of the inadequateness of pulse radiolysis protocols to produce •NO and O2•− rapidly enough to allow simple and accurate determinations of the rate constant, recommending a value of $1.6 \pm 0.3 \times 10^{10}$ M^{-1} s^{-1} that resulted from a weighted average of flash photolysis determinations that varied between $1.3 \pm 0.2 \times 10^{10}$ and $2.0 \pm 0.4 \times 10^{10}$ M^{-1} s^{-1} with different experimental designs.[13] In contrast, a flash photolysis experiment-derived value of 6.7×10^9 M^{-1} s^{-1} was previously reported by Huie and Padmaja.[9] Strikingly, no attempt has been made to understand this reaction within the theoretical field of diffusion-controlled/diffusion-influenced reactions.[14]

Contrary to what is found under physiologic conditions, ONOO− is fairly stable in the absence of H3O+, CO2, and other Lewis acids.[3] Thanks to this fact, the reverse reaction (reaction 1B) rate constant has been accurately studied in strongly alkaline aqueous media in the presence of sufficiently high concentrations of •NO and O2•− scavengers that allow the continuous monitoring of the irreversible advance of the thermohomolytic reaction.[15−18]

$$\text{ONOO}^- \rightarrow \text{•NO} + \text{O}_2^{\bullet -} \quad k_r^{irr} \qquad (1B)$$
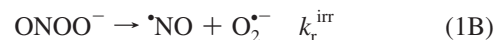
In this way, Sturzbecher and co-workers could establish the temperature (15−55 °C) and pressure (5−175 MPa) dependencies of the rate constant of reaction 1B.[18]

Thus, an equilibrium state between ONOO− and •NO, O2•− can be assumed to occur in strongly alkaline solutions (pH > 12) (eqs 2 and 3)

* To whom correspondence should be addressed. H.B.: phone, 0598-25220910 ext. 143; e-mail, hbotti@pasteur.edu.uy. R.R.: phone, 0598-29249562; e-mail: rradi@fmed.edu.uy.
† Instituto Pasteur de Montevideo.
‡ Center for Free Radical and Biomedical Research.
§ Facultad de Ciencias, Universidad de la República.
∥ Vanderbilt University.
ETH Zürich.
∇ Facultad de Medicina, Universidad de la República.
⊥ Current Address: Department of Pharmaceutical Chemistry, University of Kansas, Lawrence, Kansas 66045, United States.

Brownian Diffusion-Controlled Equilibria

J. Phys. Chem. B, Vol. 114, No. 49, 2010 **16585**

$$\cdot\text{NO} + \text{O}_2^{\cdot-} \rightleftharpoons \text{ONOO}^- \qquad (2)$$

$$K_A^{eq} = \frac{[\text{ONOO}^-]}{[\cdot\text{NO}][\text{O}_2^{\cdot-}]} \qquad (3)$$

The chemical equilibrium association constant (K_A^{eq}) and the corresponding standard Gibbs' energy of ONOO$^-$ formation have been deduced from the values of k_f^{irr} and k_r^{irr},[16−19] but suffer from the uncertainty in k_f^{irr} values

$$1.9 \times 10^{11} \text{ M}^{-1} \leq K_A = \frac{k_f^{irr}}{k_r^{irr}} \leq 1.0 \times 10^{12} \text{ M}^{-1} \qquad (4)$$

In this work we study the reversible reaction of $\cdot$NO and O$_2^{\cdot-}$ to form ONOO$^-$ (reaction 1A) by amperometrically measuring $\cdot$NO concentrations present in alkaline (pH > 12) ONOO$^-$ solutions of known concentration. This approach circumvents the problems inherent to the measurement of very high reaction rate constants and allows a simple and accurate study of this reaction−diffusion system. Some results and conclusions may be relevant beyond the physical chemistry of peroxynitrite, showing that this chemical equilibrium and the methodology we have employed can be valuable to experimentally test other predictions of the evolving theory of diffusion-controlled reversible reactions.

II. Experimental Section

High-purity poly(ethylene glycol) (PEG) 3350 and 8000 were obtained from Fluka. Sodium hydroxide, glycerol (GOL), potassium superoxide, and other chemicals were purchased at the highest purity available from Sigma-Aldrich.

Peroxynitrite was synthesized by the reaction of acidified hydrogen peroxide and nitrite in aqueous solutions by rapid mixing, controlled aging, and later quenching by a concentrated NaOH solution.[20] Peroxynitrite stock solutions (≤ 0.2 M) were stored in NaOH 0.6 M at -80 °C for less than a year and contained 0.22 mol of NO$_2^-$ per mole of synthesized ONOO$^-$. Peroxynitrite was quantified by UV−vis absorption spectrophotometry at 302 nm, using $\varepsilon = 1670$ M^{-1} cm^{-1}.[21] Highly concentrated (≤ 0.9 M) ONOO$^-$ solutions were obtained by freeze−thawing fractionation from the above-mentioned stock solutions. Samples used for flash photolysis experiments contained ca. 200 μM ONOO$^-$, synthesized according to Bohle et al.,[22,23] and less than 20 μM nitrite at pH 12. All aqueous solutions were prepared fresh using nanopure water. High-viscosity 50% and 25% glycerol solutions were prepared by mixing equal parts of NaOH (50−100 mM) and glycerol (100% and 50% in water). The relative viscosity was checked in a capillary-tube homemade viscosimeter. Alkaline solutions of PEG 4000 (25%) and 8000 (15%) were prepared in a similar way.

$\cdot$NO measurements were performed with an Apollo II $\cdot$NO gas analyzer from WPI Inc. equipped with an ISO-NO electrode as before.[24] This electrode possesses a gas-permeable membrane envelope that allows a highly specific determination of free dissolved $\cdot$NO gas concentrations ≤ 10 nM. Calibration at different temperatures and viscosities were performed using the reduction of sodium nitrite by an acidic potassium iodide solution and by addition of known amounts of an anaerobic stock solution of authentic $\cdot$NO, respectively.
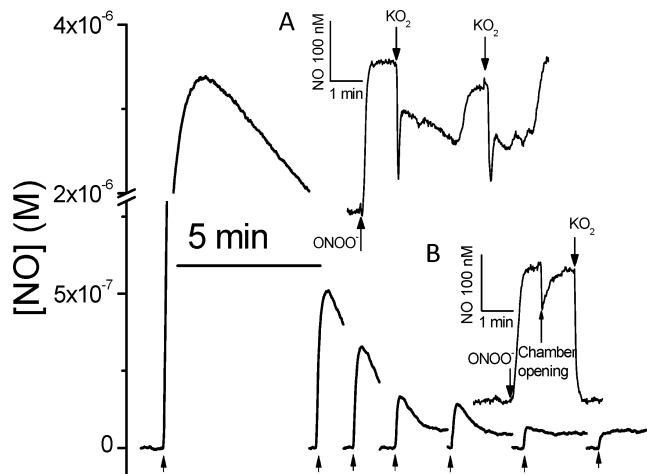
Figure 1. Stable nitric oxide concentrations in alkaline peroxynitrite solutions. Repeated sampling (up arrows) of a peroxynitrite alkaline stock solution (150 mM) was performed (1 mM ONOO$^-$, final concentration). Injection of each separate aliquot into the $\cdot$NO sensor chamber ($V = 3$ mL) containing 10 mM NaOH resulted in the appearance of amperometric signals attributable to $\cdot$NO. The alkaline peroxynitrite stock solution used was previously stored in a closed vial at -20 °C for a month, thawed at 37 °C just before measurement, and maintained open at room temperature for repeated sampling. After each addition, the $\cdot$NO time course was followed for a few minutes and then the recording was stopped. NaOH solution was changed, and the fresh solution was purged using N$_2$ gas before the recording was restarted and $\cdot$NO measurement in the ONOO$^-$ stock solution was performed ($\sim$15 min interval). $T = 34$ °C. Insets A and B: 7.5 mM peroxynitrite (final concentration) was added when indicated. Addition of a small amount of solid KO$_2$ produced a transient partial decrease of the $\cdot$NO signal (A), whereas a larger amount (B) abolished transiently the signal. The same stable $\cdot$NO concentration was recovered after these transient effects.

Laser flash photolysis experiments were performed with an Applied Photophysics LKS 50 instrument. The third harmonics (6 ns, 355 nm, 100−200 mJ/pulse) of a Nd:YAG laser (Quantel Brilliant B) was used for photolysis. To minimize photolysis of ONOO$^-$ by the analyzing light, a long-pass cutoff filter with a half-maximum absorption at 325 nm was placed between the cuvette and the Xe lamp. Signals were recorded with a LeCroy WaveRunner 64Xi digital oscilloscope at 335 nm. For temperature stabilization a water thermostat was used. Solutions were evacuated and flushed with argon repeatedly in a 1 cm quartz fluorescence cell from Hellma GmbH fitted with a Young valve. For determination of k_f^{irr} an extinction coefficient at 335 nm of 1000 M^{-1} cm^{-1} for ONOO$^-$ was used.

III. Results

A. Direct Measurement of $\cdot$NO in Equilibrium with ONOO$^-$ in Alkaline Stable ONOO$^-$ Solutions. Stable $\cdot$NO concentrations can be measured if aliquots of peroxynitrite from a concentrated alkaline stock solution are injected in the $\cdot$NO sensor chamber previously filled with freshly prepared 50 mM $\leq$ NaOH $\leq$ 10 mM. Nevertheless, some recently and rapidly thawed concentrated peroxynitrite stock solutions may contain higher than equilibrium $\cdot$NO concentrations, as shown in Figure 1. Higher than equilibrium $\cdot$NO concentrations are also observed if aqueous $\cdot$NO is added to ONOO$^-$ solutions. Given enough time, the concentration of $\cdot$NO reaches a lower stable value in the vial. In the experiment of Figure 1, the initial measured $\cdot$NO concentration in the sensor chamber was 3.35 μM and the final stable $\cdot$NO concentration (maintaining the vial of the stock solution opened for 1.5 h at room temperature) was 56 $\pm$ 4 nM

(1 mM ONOO⁻, $T = 34$ °C, Figure 1). Purging of ONOO⁻ stock solutions with N₂ gas prior to injection of ONOO⁻ in the ·NO sensor chamber prevents the observation of the higher initial concentrations but does not alter the final stable measured ·NO concentration, which supports that ·NO is not just a residual contaminant of ONOO⁻ solutions but that it is continuously formed from ONOO⁻ through reaction 1B. The fact that a stable concentration of ·NO was measured suggests that an equilibrium condition was rapidly reached in the ·NO sensor chamber after diluting the stock peroxynitrite solution. We reasoned that this putative equilibrium condition should also involve $O_2^{·-}$. Addition of solid KO₂ (∼5−20 mg, 90−375 mM) to 7.5 mM ONOO⁻ (37 °C) led to a transient decrease in the ·NO concentration, after which the previous stable concentration of ·NO was recovered (Figure 1, insets A and B). Careful observation showed that the fine bubbling (due to $O_2^{·-}$ dismutation) that started immediately after addition of solid KO₂ ceased synchronically with spontaneous recovery of the ·NO signal. This shows that $O_2^{·-}$ concentrations higher than those of ·NO were attained transitorily and caused the observed decreased of ·NO concentrations; this decrease is surely due to ONOO⁻ formation (ΔONOO⁻ = −Δ·NO).

Considering that (a) the instantaneous concentration of ·NO depends on the concentration of $O_2^{·-}$, (b) both ·NO and $O_2^{·-}$ are continuously formed by ONOO⁻ homolysis, (c) ONOO⁻ homolysis and ·NO recombination with $O_2^{·-}$ are the principal reaction fluxes in the system, (d) in the conditions tested ONOO⁻ is stable, and (e) excess concentrations of ·NO or $O_2^{·-}$ over that of $O_2^{·-}$ or ·NO (respectively) are cleared by other minor reaction channels (i.e., $O_2^{·-}$ dismutation, ·NO autoxidation; see discussion section) then if a stable concentration of ·NO is reached, the concentration of $O_2^{·-}$ should also be stable and equal to that of ·NO. Therefore, the equilibrium constant can be calculated according to eq 5

$$K_A^{eq} \equiv \frac{[ONOO^-]_{eq}}{[·NO]_{eq}[O_2^{·-}]_{eq}} = \frac{[ONOO^-]_0}{([·NO]_{eq})^2} \qquad (5)$$

Since in our conditions $[·NO]_{eq} \ll [ONOO^-]_0$, in eq 5 we make the simplification that the concentration of peroxynitrite is fixed and equal to that calculated from the dilution made from the stock solution (as usually assumed). From the experiment shown in Figure 1, we calculate the equilibrium constant K_A^{eq} for the formation of ONOO⁻ at 34 °C: $K_A^{eq} \simeq 3.2 \times 10^{11}$ M⁻¹. We discarded the possibility that the rates of ONOO⁻ decomposition at pH > 12 could significantly affect the observed equilibrium condition (Supporting Information). As controls, equivalent amounts of nitrate, nitrite, or decomposed peroxynitrite (peroxynitrite reverse-addition test) were injected, but no signal was observed (not shown).

B. Dependence of K_A^{eq} on Viscosity and Temperature. Current knowledge about the back reaction as characterized by k_r^{irr} [16−19] clearly shows that it is activation controlled. Therefore, if the reaction of ·NO with $O_2^{·-}$ to give ONOO⁻ (characterized by k_f^1) is diffusion limited and if the physicochemical process is elemental, then, in agreement with Stokes−Einstein and Smoluchowski equations (eqs 6 and 7, respectively),[14] an increase in the viscosity (η) should decrease k_f^1, and leave k_r^1 unchanged, thus, which would result in a decrease in the equilibrium constant in accordance with eq 8 and an increase in measured ·NO concentration in agreement with eq 5

$$D_i = \frac{k_B T}{6\pi\eta R_{hyd}} \qquad (6)$$

$$k_{Smol} = \frac{N_A 4\pi R^* D_{ij}}{1000} \qquad (7)$$

$$K_A^{Smol} = \frac{k_{Smol}}{k_b^1} = \frac{N_A 4\pi R^* D_{ij}}{1000 k_b^1} \qquad (8)$$

In eqs 6−8, R_{hyd} is the hydrodynamic radius, N_A is Avogadro's number, k_B is the Boltzmann constant, R^* is the effective reaction distance, and $D_{ij} = D_{·NO} + D_{O_2^{·-}}$ is the sum of the solute−solvent diffusion coefficients of the reactive pair (diffusion coefficient of relative motion).

To test if the observed value of the apparent equilibrium constant K_A^{eq} depends on η, the concentration of ·NO in apparent equilibrium with peroxynitrite (7.5 mM, 25 °C) was determined in 28 (control) and 28 mM NaOH with 50% (w/v) glycerol ($\eta_{50\%GLO}/\eta_{H_2O} \simeq 4$). Two processes take place in the presence of high concentrations of glycerol: a fast one that was complete in seconds (also present in the control experiment) and a slow one that caused a progressive accumulation of ·NO (see Supporting Information). This last process was accompanied by peroxynitrite decay as followed at 302 nm in a UV spectrophotometer (not shown). A similar behavior was observed when polyethylene glycol (PEG) 3350, PEG 8000, or nitroblue tetrazolium (NBT²⁺) was used, which suggests that all of these agents were promoting ·NO formation from ONOO⁻ (Supporting Information). Therefore, if the plot curves are corrected for the mentioned unwanted slow reaction (Supporting Information), the effect of increasing η over ·NO in equilibrium with peroxynitrite and therefore over K_A^{eq} is negligible (as shown in Figure 2A). Consider that if only k_f is diffusion-limited and since the viscosity of the used solution is approximately 4 times that of the control media, the expected change for the diffusion-dependent equilibrium is an increase in the measured ·NO concentration of approximately 2 times (proportional to $(1/\eta)^{1/2}$). This result supports any of three contentions: (a) neither k_r^{eq} nor k_f^{eq} are diffusion influenced, (b) both are diffusion controlled, or (c) the process is complex involving both diffusional and activational steps in the backward direction and at least a diffusional step in the forward direction. Since as already mentioned the rate constant of ONOO⁻ homolysis is well known to be thermally activated, possibility b can be disregarded. Since the reported values of k_f^{eq} are close to the irreversible steady-state diffusion limit imposed by k_f^{Smol}, possibility a can be disregarded as well. Therefore, we conclude that the equilibrium under study is more likely to behave as proposed in option c, which supports that the physicochemical process studied at equilibrium might be better described by a more complex than previously thought mechanism. In general, the nondiffusional steps are not necessarily activational (speeded by raising the temperature), since nonactivational processes might influence the rate of the reaction as well, including spin conversion, steric factors, in-cage dynamics, microscopic hydrodynamic effects.[25−28]

Next, we study the dependence of K_A^{eq} on the temperature (15−50 °C, at 1 atm constant pressure), and in the subsequent section we study the dependence of the forward rate constant on the temperature. Following a Van't Hoff analysis (eqs 9A and 9B),[29] we plot $\ln(K_A^{eq})$ vs T^{-1} (Figure 2B). The concentration of ONOO⁻ was kept constant at 5.1 mM. The straight line represents the best-fit curve for a linear model (eqs 9A and 9B).

Brownian Diffusion-Controlled Equilibria

J. Phys. Chem. B, Vol. 114, No. 49, 2010 **16587**
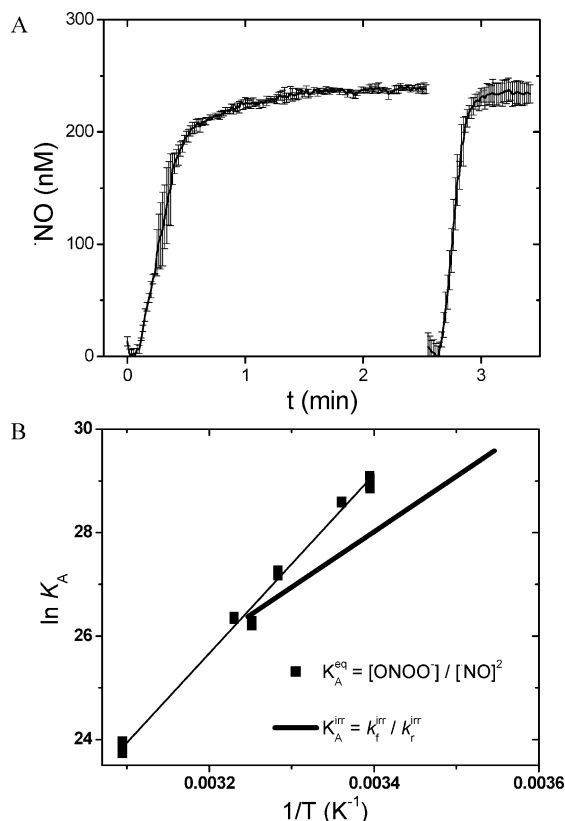
Figure 2. Dependence of K_A on η and T. (A) Nitric oxide concentrations in equilibrium with alkaline peroxynitrite (7.5 mM) are measured in the absence (trace on the left) and presence (trace on the right) of 50% glycerol. Averages $\pm$ SD are displayed, $n = 3$; results representative of two separate experiments. (B) Plots of $\ln K_A$ as a function of T^{-1}. The values of K_A at equilibrium (closed squares) were calculated using eq 5. The concentration of $[ONOO^-]_{eq}$ was kept constant at 5.1 ± 0.1 mM, and the resuting $[\bullet NO]_{eq}$ varied from $\simeq 40$ nM at 22 °C to $\simeq 470$ nM at 55 °C. The thick line represents the calculated values of K_A from independently determined rate constants in irreversible conditions (k_f determined in this work by flash photolysis (see below), and k_r was determined by stopped-flow spectrophotometry Sturzbecher et al.[18]

$$\ln K_A^{eq} = \frac{d \ln K_A^{eq}}{d\,T^{-1}}\left(\frac{1}{T}\right) + \frac{\Delta_r S}{R} = \ln K_A^{eq} =$$

$$\frac{(17.3 \pm 0.4) \times 10^3}{T} - 29.6(\pm 1.4) \quad (9A)$$

Where the slope

$$\frac{d \ln K_A^{eq}}{d\,T^{-1}} = -\frac{\Delta_r H^\circ}{R} = (17.3 \pm 0.4) \times 10^3 \quad (9B)$$

Hence, we calculate

$$\Delta_r H^\circ = -R(1.73 \times 10^4 \pm 427K) = -144(\pm 4) \text{ kJ mol}^{-1} \quad (10)$$

And

$$\Delta S_r^\circ = R(-29.6) = -246(\pm 12) \text{ J mol}^{-1}\,\text{K}^{-1} \quad (11)$$

Evaluation of ΔG° at 25 °C gives

$$\Delta_r G^\circ = \Delta_r H^\circ - T\Delta_r S^\circ = -70(\pm 5) \text{ kJ mol}^{-1} \quad (12)$$

The obtained value of ΔG° is in good agreement with values from -64.4 to -68.5 kJ mol^{-1} that can be deduced from reported values of k_r^{irr} and k_f^{irr} (referenced in the Introduction).

C. Dependence of k_f^{eq}, k_f^{irr}, k_f^{Smol}, and D_{NO} on Temperature. If we assume that the activation-controlled reverse reaction rate constant is the same whether it is determined in equilibrium or in irreversible conditions, then taking $k_r^{irr} = 0.02$ s^{-1} at 25 °C from the literature[16,18] and using $K_A^{eq} = 2.03 \times 10^{12}$ M^{-1} (eq 9A), we calculate a value of $k_f^{eq} = 3.2 \times 10^{10}$ M^{-1} s^{-1} at 298.15 K (eq 13A)

$$k_f^{eq} = K_A^{eq} k_r^{irr} \quad (13A)$$

The calculated value is above the classical diffusion limit (see below, eqs 15A and 15B) and in good agreement with the higher values reported by Kissner et al. and Nauser et al.[12,13] Assuming the validity of this relationship for any temperature within the studied range (eq 13B) and combining our data with the data on the dependence of k_r^{irr} on the temperature as reported by Sturzbecher et al.,[18] we deduced k_f^{eq} as a function of T (eqs 13C and 13D)

$$\ln k_r^{eq} = \ln k_r^{irr} = 37.02 - \frac{(12.3 \pm 0.2) \times 10^3}{T} \quad (13B)$$

$$\ln K_A^{eq} = -29.6(\pm 1.4) + \frac{(17.3 \pm 0.4) \times 10^3}{T} =$$
$$\ln\left(\frac{k_f^{eq}}{k_r^{eq}}\right) = \ln k_f^{eq} - \ln k_r^{eq} \quad (13C)$$

$$\ln k_f^{eq} = \ln K_A^{eq} + \ln k_r^{eq} = -29.6 + \frac{(17.3 \pm 0.4) \times 10^3}{T} +$$
$$37.0 - \frac{(12.3 \pm 0.2) \times 10^3}{T} =$$
$$7.4 + \frac{(5.0 \pm 0.7) \times 10^3}{T} \quad (13D)$$

Accordingly, the expected rate constant value at 37 °C and $[ONOO^-] = 5.2$ mM is $k_f^{eq} = 1.7 \times 10^{10}$ M^{-1} s^{-1}. The values of $\ln k_f^{eq}$ plotted against $1/T$ (Arrhenius plot) are shown in Figure 3 (squares, left y axis). Data on $\ln k_f^{eq}$ vs $1/T$ can be fitted to the Arrhenius equation, yielding negative and apparently constant values of activation energy $E_a = -40 \pm 6$ kJ mol^{-1} and a very low pre-exponential factor $A = 1.70 \times 10^3$ M^{-1} s^{-1}.

The rate constant for the reaction of $\bullet NO$ and $O_2^{\bullet-}$ under irreversible conditions (k_f^{irr}) was studied by flash photolysis of alkaline $ONOO^-$ solutions as a function of the temperature (Figure 3, triangles, left y axis). The observed values of k_f^{irr} are in excellent agreement with previous flash photolysis determinations.[12,13] The value of k_f^{irr} varied from 1.07×10^{10} to 1.71×10^{10} M^{-1} s^{-1} on going from 282.15 to 308.15 K. A very good fit to the Arrhenius equation can be observed in the studied range of temperature, with positive and apparently constant $E_a = 12.9 \pm 0.6$ kJmol^{-1}, with a pre-exponential value $A = 2.70 \times 10^{12}$.
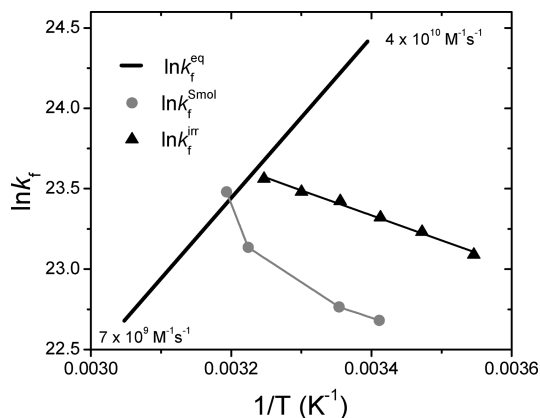
Figure 3. Arrhenius plots for the rate constant of the reaction of ˙NO with $O_2^{˙-}$ under equilibrium and irreversible conditions. The rate constant for the reaction of ˙NO with $O_2^{˙-}$ under irreversible conditions (k_f^{irr}) was directly determined by flash photolysis as a function of the temperature (triangles). The values of k_f^{eq} were deduced from K_A and k_r^{irr} as explained in the text (thick line, the extreme values are indicated for direct reference). The values of the diffusion-limited rate constant according to the steady-state irreversible Smoluchowski theory k_f^{Smol} are displayed as gray circles (using reported diffusion coefficients for ˙NO).

In addition, we studied the dependence on temperature of the diffusion coefficient of ˙NO ($D_{˙NO}$) in aqueous solution and the calculated diffusion-controlled rate constant for the irreversible steady-state advance of the reaction (k_f^{Smol}) using the four reported values of $D_{˙NO}$: 2.07×10^{-5} cm^2 s^{-1} at 20 °C, 2.21×10^{-5} cm^2 s^{-1} at 25 °C,[30] 3.3×10^{-5} cm^2 s^{-1} at 37 °C,[31] and 5.10×10^{-5} cm^2 s^{-1} at 40 °C.[32] The dependence of $D_{˙NO}$ on the temperature (Supporting Information) is in very good agreement with that predicted by the Stokes−Einstein relationship (eq 14)

$$D_{NO} = \frac{k_B T}{\xi_{˙NO}} = \frac{k_B T}{6\pi(\eta^{\alpha_{˙NO}})R_{hyd}} \quad (14)$$

Regarding eq 14, the reported values of $D_{˙NO}$ can be explained with a narrow range of values of $\alpha_{˙NO}$ ($1.05 \leq \alpha_{˙NO} \leq 1.12$), showing that the diffusion of ˙NO in aqueous media is quasi-stokessian ($\alpha \equiv 1$ for a strictly stokessian diffusion). This is in agreement with a previous report[33] and expectedly departs from the behavior of ˙NO in lipid environments ($\alpha \simeq 0.5$)[24] and of dioxygen in *n*-alkanes.[34] Figure 3 (squares, left *y* axis) also shows the dependence on the temperature of the diffusion-limited rate constant for the reaction of ˙NO with $O_2^{˙-}$ to give ONOO$^-$ as if it would obey the steady-state Smoluchowski relationship (eqs 6 and 7), calculated using $\alpha_{˙NO} = 1.08$. The dependence on the temperature of the diffusion coefficient of $O_2^{˙-}$ is not known. Nevertheless, if we assume that $\alpha_{O_2^{˙-}} = 1$ (a likely safe assumption), the effect of changes in *T* (and concomitantly in η) on the calculated diffusion-limited rate constant for the reaction of ˙NO with $O_2^{˙-}$ can be evaluated (eq 15A)[14]

$$k_f^{Smol} = 4\pi \frac{N_A}{1000}(R^*)\left[\left(\frac{k_B T}{6\pi}\right)\left(\frac{1}{R_{˙NO}^{hyd}\eta^{\alpha_{˙NO}}} + \frac{1}{R_{O_2^{˙-}}^{hyd}\eta^{\alpha_{O_2^{˙-}}}}\right)\right] \quad (15A)$$

We assume that the reactive pair is a van der Waals contact pair as expected for a covalent reaction, giving $R^* = R_{˙NO}^{vdW}$

$+ R_{O_2^{˙-}}^{vdW} \simeq 3.2 \times 10^{-8}$ cm. Taking $R_{˙NO}^{hyd} = R_{˙NO}^{vdW}$ and $R_{O_2^{˙-}}^{hyd} = 2.05 \times 10^{-8}$ cm as used previously,[35] calculation of k_f^{Smol} at 25 °C gives

$$k_f^{Smol(298.15K)} = \left(\frac{4\pi N_A}{1000}\right)(2.2 \times 10^{-5} \text{ cm}^2 \text{ s}^{-1} +$$
$$1.2 \times 10^{-5} \text{ cm}^2 \text{ s}^{-1}) \times (1.6 \times 10^{-8} \text{ cm} +$$
$$2.05 \times 10^{-8} \text{ cm})$$
$$= 9.4 \times 10^9 \text{ M}^{-1} \text{ s}^{-1} \quad (15B)$$

Contrary to the linear behavior of $\ln k_f^{eq}$ and $\ln k_f^{irr}$, nonconstant positive values of E_a are needed to explain results on $\ln k_f^{Smol}$ (the calculated steady-state Smoluchowski constant) vs $1/T$ in the range of *T* under consideration (see Discussion).

From Figure 3 it can be observed that (a) the forward reaction rate constant as described by $k_f^{eq} = K_A^{eq} k_r^{irr}$ does not behave as expected for the case of the calculated Smoluchowski steady-state diffusion-limited reaction rate constant (which is typically assumed to be valid for irreversible reactions), (b) neither does k_f^{irr} follow k_f^{Smol} behavior, and (c) the temperature dependence of k_f^{Smol} follows the same temperature dependence as $D_{˙NO}$ (Figure 3).

D. Dependence of K_A and k_f^{eq} on ONOO$^-$ Concentration. We determined the concentrations of ˙NO in apparent equilibrium with ONOO$^-$ as a function of ONOO$^-$ concentration at 37 °C in NaOH 50 mM (Figure 4A). Our initial goal was to better evaluate K_A and to confirm the expected linear relationship between the square of the ˙NO concentration and the concentration of ONOO$^-$. This expected linear relationship would imply a constant K_D (eq 16)

$$K_D^{eq} = K_A^{eq-1} = \frac{([˙NO]_e)^2}{[ONOO^-]_0} = \frac{d([˙NO]_e)^2}{d[ONOO^-]_0} = \text{constant} \quad (16)$$

If K_D = constant, the applicability of the mass-action law to the case under study is warranted. However, the measured ˙NO concentration deviated (downward) as the concentration of ONOO$^-$ increased, which indicates that K_D (and K_A) depends on ONOO$^-$ concentration. To our knowledge, this kind of behavior has not been previously observed, but deviations from the mass-action law have been theoretically predicted for diffusion-influenced reactions in reversible stable conditions (see Discussion).[36−40] As a control we studied the dependence of the ˙NO signal for a known amount of authentic ˙NO on the ionic strength by using 25 mM NaOH with or without 0.1 M NaCl or 0.1 M NaOH and observed just a little increase in the signal (not shown). Thus, the increase of ionic strength in the sensor chamber was not responsible for the observed reduction on ˙NO with increasing ONOO$^-$ concentrations. We degassed the NaOH solutions immediately prior to use (by heating) and repeated the experiment at high ONOO$^-$ concentration, but no change was observed. In addition, it can be ruled out that increased $O_2^{˙-}$ dismutation could cause the observed effect, because lowering $O_2^{˙-}$ would increase (not decrease) ˙NO concentration. Finally, we also considered the possibility of a reaction between ˙NO and ONOO$^-$ or ONOO$^-$-derived reactive species. However, estimates for the direct reaction rate constant are smaller than 1.3×10^{-3} M^{-1} s^{-1}.[41,42] The maximal concentration of ˙NO measured after bolus addition of aqueous

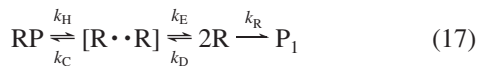Brownian Diffusion-Controlled Equilibria

J. Phys. Chem. B, Vol. 114, No. 49, 2010 **16589**
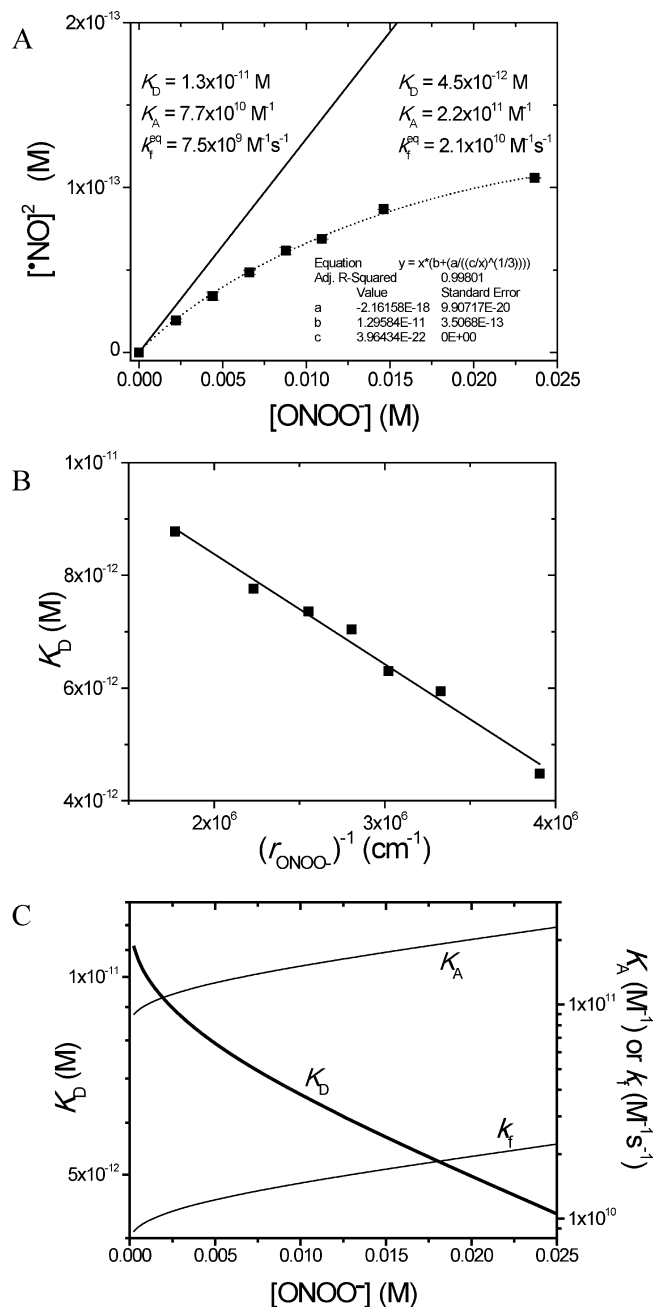
Figure 4. Dependence of K_A and k_f^{eq} on ONOO$^-$ concentration. Measured $^\bullet$NO in apparent equilibrium with alkaline ONOO$^-$ solutions at different ONOO$^-$ concentrations (37 °C, pH >12.5). (A) The squares of the values of the observed $^\bullet$NO concentrations were plotted against the corresponding ONOO$^-$ concentrations (closed squares ± SE). The dotted curve and values displayed below result from a least-squares fitting of parameters in eq 28B to the experimental data (parameters "a" and "b" were adjusted, while parameter "c" was kept constant ($c = 3000/4\pi N_A$). The continuous trace is $[^\bullet NO]^2 = b[ONOO^-]$, which is asymptotic to the dotted curve when $[ONOO^-] \to 0$. The values above the solid line represent this linear behavior. The higher observed value of $k_f^{eq} = 2.1 \times 10^{10}$ M^{-1} s^{-1} obtained at high $[ONOO^-]$ is indicated, together with the corresponding values of K_D and K_A. For calculations we used $k_r^{irr}{}_{(37\ °C)} = 0.097$ s^{-1} (Sturzbecher, 2007). (B) Plot of experimental values of K_D as a function of the inverse of the calculated r, where r is the average distance between ONOO$^-$ molecules. The best fit to a linear equation gives $y_{(x=0)} = b = 1.23 \times 10^{-11}$ M and a slope $a = -1.95 \times 10^{-18}$ M cm^{-1}, similar to the values obtained by directly fitting eq 28B to experimental data in A. (C) Calculated values of K_D^{eq}, K_A^{eq}, and k_f^{eq}, according to A and eqs 28A–C, plotted against $[ONOO^-]$.

$^\bullet$NO decreased in the presence of ONOO$^-$ in a constant proportion for a given ONOO$^-$ concentration; ONOO$^-$ addition accelerated the rate of decay of authentic $^\bullet$NO in alkaline conditions (NaOH 50 mM), and this reaction was linearly dependent on ONOO$^-$ concentration with an apparent rate constant of ~4×10^{-6} s^{-1} (not shown). This rate constant and the rate constant of ONOO$^-$ decay in similar conditions (Supporting Information) are 3−4 orders of magnitude smaller than the rate constant of $^\bullet$NO and O$_2^{\bullet-}$ formation from ONOO$^-$ at equilibrium through reaction 1B, and hence, they have a negligible influence in the stationary state under study (a chemical equilibrium). Importantly, if our assumptions are correct and the determinations we made actually reflect the free $^\bullet$NO concentrations in equilibrium with ONOO$^-$ and O$_2^{\bullet-}$, the increment of K_A values with ONOO$^-$ concentration means that a nonconstant rate coefficient between $^\bullet$NO and O$_2^{\bullet-}$ can be deduced, as shown in Figure 4C. As discussed below, this is likely caused by a space (distance) dependence of k_f^{eq} and the equilibrium constants, as proposed in Figure 4B and in eqs 21A−C. The higher experimental k_f^{eq} value that we obtained at high $[ONOO^-]$ and 37 °C is 2.1×10^{10} M^{-1} s^{-1}, which is in agreement with the higher values reported by Kissner et al. and Nauser et al.[12,13] The minimum observed value $k_f^{eq} = 7.5 \times 10^9$ M^{-1} s^{-1} at 37 °C was estimated by derivation at $[ONOO^-] \to 0$ using eq 21A fitted to the experimental results of Figure 4A and is in good agreement with the value reported by Huie et al. (6.7×10^9 M^{-1} s^{-1}).[9]
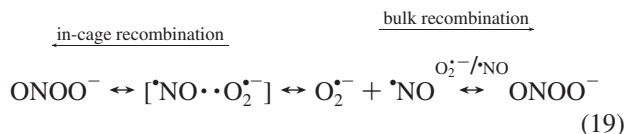
IV. Discussion

A. Simple and Known Chemistry Going on in the System under Study. There is already a vast accumulated knowledge about peroxynitrite chemistry.[7] Importantly, the reaction of $^\bullet$NO and O$_2^{\bullet-}$ gives only ONOO$^-$ and vice versa,[43] and since neither ONOO$^-$, $^\bullet$NO, or O$_2^{\bullet-}$ dimerization nor any other reaction takes place to any significant extent (see Supporting Information and discussion below), the chemical system is correctly described in terms of a simple reaction of the A + B = C type. Considering the widely recognized stability of ONOO$^-$ at pH > 12[21,43−45] (see also data on ONOO$^-$ stability in alkaline conditions in the Supporting Information), the observed stability of $^\bullet$NO concentrations in alkaline ONOO$^-$ solutions clearly indicates that we are witnessing the equilibrium between ONOO$^-$, $^\bullet$NO, and O$_2^{\bullet-}$. Adding $^\bullet$NO or O$_2^{\bullet-}$ from an external source perturbs the equilibrium, but given enough time, the system returns to the previous equilibrium concentrations (Figure 1). The return to the previous equilibrium state despite addition of $^\bullet$NO or O$_2^{\bullet-}$ is the only way in which known minor reaction pathways manifest themselves. These almost undetectable pathways include ONOOH formation ($pK_a = 6.8$) and decay,[45] uncatalyzed O$_2^{\bullet-}$ dismutation,[46] $^\bullet$NO diffusion out of the solution, and $^\bullet$NO autoxidation.[11,47] Therefore, the chemical simplicity and stability of the system are the key ingredients that make this study possible and make the system a good candidate for further testing kinetics and thermodynamics hypothesis of general relevance.

B. Dependence of K_{eq} on ONOO$^-$ Concentration Arises from the Dependency of k_f^{eq} on Distance. If the law of mass action applies, eq 16 should hold. Instead, we found a nonlinear dependence of $([^\bullet NO]_e)^2$ on $[ONOO^-]_e$ (Figure 4). The Franck−Rabinowitch effect describes irreversible radical generation and recombination processes in a simple form (eqs 17 and 18)

$$RP \underset{k_C}{\overset{k_H}{\rightleftharpoons}} [R \cdot \cdot R] \underset{k_D}{\overset{k_E}{\rightleftharpoons}} 2R \overset{k_R}{\longrightarrow} P_1 \qquad (17)$$

$$F_C = k_C/(k_C + k_E) \qquad (18)$$

where F_C is the fraction of radicals that undergo geminate radical pair recombination within the solvent cage. As applied to the specific process under consideration, the model can be represented according to eq 19

in-cage recombination   bulk recombination

$$ONOO^- \leftrightarrow [^\bullet NO \cdot \cdot O_2^{\bullet-}] \leftrightarrow O_2^{\bullet-} + {}^\bullet NO \overset{O_2^{\bullet-}/^\bullet NO}{\leftrightarrow} ONOO^- \qquad (19)$$

The effective dissociation rate constant k_r^{eff} can be expressed as shown below (eq 20)

$$k_r^{eff} = k_H(1 - F_C) = k_H - \frac{k_H k_C}{k_C + k_E} \qquad (20)$$

According to experimental data[18] k_r^{eff} and therefore k_H, k_C, and k_E are independent of $ONOO^-$ concentration. Therefore, we can state that $k_r^{eff} = k_r^{irr} = k_r^{eq}$.

Other possibilities that should be ruled out are $ONOO^-$, ${}^\bullet NO$, or $O_2^{\bullet-}$ dimerizations, as they can be the cause of apparent deviations from the law of mass action (mainly $ONOO^-$ dimerization). The rates of $ONOO^-$ decay at alkaline pH in the presence[18] or absence (Supporting Information) of suitable concentrations of ${}^\bullet NO$ and $O_2^{\bullet-}$ scavengers depend linearly on $[ONOO^-]_0$; therefore, any significant $ONOO^-$ dimerization can be discarded. In this regard, it should be clarified that in a recent report entitled "Dimeric form of peroxynitrite", Simon and Tulub simulate the formation in the gas phase of a loosely bound $O_2^{\bullet-} \cdots {}^\bullet NO$ triplet heterodimer but not the production of a $ONOO^- \cdots ONOO^-$ dimer as the title indicates.[48] Nitric oxide dimerization can occur in the gas phase,[49-51] but calibration curves show a strictly linear signal dependence on added ${}^\bullet NO$ at all tested concentrations (0.01–2.00 μM, not shown). Finally, to the best of our knowledge, $O_2^{\bullet-}$ dimerization has never been observed or proposed to occur in any condition and should cause an upward curvature of $([{}^\bullet NO]_{eq})^2$ vs $[ONOO^-]_{eq}$, which would be in contrast to what we observed (Figure 4A).

The departure from ideal solution conditions may also be considered as a cause, at least in part, for the observed deviation from the law of mass action. This deviation would apply to the more concentrated species, $ONOO^-$. Nevertheless, by taking as reference the behavior of KNO_3,[52] it can be estimated that at the highest $ONOO^-$ concentration used in the experiments shown in Figure 4 (25 mM), the activity coefficient might have changed by less than 12% with respect to the usual Henry's law limiting value of $\gamma_2 = 1$ when the mole fraction of the solute $(X_2) \to 0$. In addition, no effect of changes in the ionic strength (I) on the rate constant of the reaction of ${}^\bullet NO$ and $O_2^{\bullet-}$ and on the rate constant of $ONOO^-$ homolysis have been observed previously.[11,18]

Having discarded the above-mentioned confounding factors we conclude that the concentration dependence of K_D^{eq} (Figure 4A) should be the consequence of changes in k_f^{eq} (Figure 4B and 4C). Below we propose a phenomenological expression to account for the concentration–distance dependence of K_D^{eq} (eq

21A) and hence of $[{}^\bullet NO]^2$ (eq 21B, Figure 4A) and k_f^{eq} (eq 21C, Figure 4C). Derivation of these equations is based on eq 13A and on the suspected dependence of K_D^{eq} on $1/r_{ONOO^-}$ (Figure 4B)

$$K_D^{eq} = K_D^{[ONOO^-] \to 0} + \left(\frac{a}{r_{ONOO^-}}\right) =$$

$$K_D^{[ONOO^-] \to 0} + \left(\frac{a}{(3000/4\pi N_A [ONOO^-])^{1/3}}\right) =$$

$$b + \left(\frac{a}{(c/[ONOO^-])^{1/3}}\right) \qquad (21A)$$

$$[{}^\bullet NO]^2 = K_D^{eq}[ONOO^-] \qquad (21B)$$

$$(k_f^{eq})^{-1} = (k_f^{[ONOO^-] \to 0})^{-1} + \left(\frac{a}{k_r^{irr}(c/[ONOO^-])^{1/3}}\right) = \frac{b}{k_r^{irr}} + \left(\frac{a}{k_r^{irr}(c/[ONOO^-])^{1/3}}\right) \qquad (21C)$$

where a is the slope of the linear regression of K_D^{eq} over $1/r_{ONOO^-}$ shown in Figure 4B. This parameter was more reliably estimated by fitting experimental data of Figure 4A to eq 21C, giving $a = -2.16 \pm 0.1 \times 10^{-18}$ M cm. Since $a < 0$, $k_f^{eq} \geq k_f^{[ONOO^-] \to 0}$. The results shown in Figure 4 and eqs 21A–21C are in close agreement with Voituriez et al. proposals.[38,39] The observed dependence of K_D^{eq} on $ONOO^-$ concentration allowed us to deduce a range of k_f^{eq} values 7.5–21 × 10^9 M^{-1} s^{-1} for the studied $ONOO^-$ concentrations (Figure 4C). Equation 21C assumes that the reaction is completely diffusion limited, with no evidence of activation dependence. Equation 21C predicts that $K_D^{eq} \to 0$ and $k_f^1 \to +\infty$ when $[ONOO^-] \simeq 0.085$ M and $r_{ONOO^-} \simeq 1.6 \times 10^{-7}$ cm, a distance equivalent to approximately $4R^*$ or 5.5 times the distance between N and O atoms in the triplet heterodimer $O_2^{\bullet-} \cdots {}^\bullet NO$ proposed to occur in the gas phase.[48] We propose that the observed increase in K_A^{eq} with $ONOO^-$ concentration arises because the intertwined actions on k_f^{eq} of spatiotemporal correlation between newly born ${}^\bullet NO$ and $O_2^{\bullet-}$ particles (that creates a fluctuating ordering of reactants) and many body effects on radical recombinations (that result from the higher probability of nongeminate recombinations as the distance between ${}^\bullet NO$ and $O_2^{\bullet-}$ sources decrease). This would be similar to the interplay of geminate and bulk recombinations proposed by of Lee et al.,[53] although they studied systems undergoing irreversible processes and did not report any deviation from the mass action law.[53] Together, these factors determine a decrease in the macroscopic diffusional resistance for recombination of radicals (an increased time-space-averaged rate constant) as $[ONOO^-]_{eq}$ increases. It should be emphasized that while reactions in the system have correlating effects, diffusion has the opposite effect.[54] The results support that the magnitude of the later may depend on the average distance between reactants.

C. Dependence of k_f^{eq} on $[ONOO^-]_{eq}$ Unravels the Reason for Discrepancies between Previous Flash Photolysis Rate Constants. Our ultimate goal is to better understand the kinetic mechanism of formation of $ONOO^-$ from ${}^\bullet NO$ and $O_2^{\bullet-}$ in aqueous solution and if possible extract general conclusions about reversible diffusion-controlled reactions. Previous flash photolysis results[9,12,13] and the equilibrium experiments reported herein have shown a remarkable coincidence with respect to

Brownian Diffusion-Controlled Equilibria

J. Phys. Chem. B, Vol. 114, No. 49, 2010 **16591**

the observed range of forward rate constants ($6.7 \leq k_f^{irr} \leq 20 \times 10^9$ M^{-1} s^{-1} [9,12,13] versus $7.5 \leq k_f^{eq} \leq 21 \times 10^9$ M^{-1} s^{-1}). Therefore, it is very likely that the observed variations in k_f^{irr} and k_f^{eq} do actually have the same cause (the dependence of k_f on the distance between reactants). In our understanding, the time course of a diffusion-controlled reaction can be divided in at least four stages. Its very beginning and course when close to the equilibrium position have received a great deal of attention both theoretically and experimentally[55] because if nonexponential dynamics are there observed, they can be considered as diagnostics of diffusion control. The time-dependent Smoluchowski rate constant (eq 22)

$$k_f^{Smol}(t) = k_f^{Smol}\left[1 + \frac{R^*}{(\pi(D_{eff})t)^{1/2}}\right] \qquad (22)$$

uses the static target and pseudo-first-order simplifications, neglecting the possibility of a back reaction from products,[14] to account for the changes in reactant concentration at the early stage of a far from equilibrium diffusion-controlled reaction, which can be considered irreversible because the forward flux is infinitely higher than the reverse flux. These simplifications continue to be useful in the pseudo-first-order regime. According to Zeldovich−Ovchinnikov−Oshanin−Burlatzky (ZOOB) theory[36−39,54,56,57] reaction dynamics at equilibrium are dominated by fluctuational changes, and accordingly, the return after a small perturbation or progress to the equilibrium concentration of the reactant B should be in agreement with eq 23, where $B(\infty)$ is the stationary concentration of B, the dimensionless parameter $\alpha \simeq 1$, and $B(0) = 0$, $A(0) \simeq A(\infty) \gg B(\infty)$[54]

$$B(t) = B(\infty) - \frac{\alpha}{(D^{3/2}t^{3/2})} \qquad (23)$$

In this and previous works,[9,12,13] the final and intermediate stages of the diffusion-controlled reaction of $^\bullet$NO and $O_2^{\bullet-}$ have been studied. Our results on the equilibrium stage (Figure 4) agree with the prediction of distance-dependent rate constants of ZOOB theory.[38,39] Most predictions of ZOOB and other analytic theories have been tested against numerical simulations and excited-states reactions.[58,59] In this work, we demonstrate that the ground-state reaction of $^\bullet$NO and $O_2^{\bullet-}$ is actually diffusion-controlled and that changing ONOO$^-$ concentration uncovers departures from the law of mass action (Figure 4), which confirms for the first time experimentally one of the key predictions of the ZOOB theory, namely that a wide range of macroscopic forward rate constants should be observed in a diffusion-controlled reversible reaction at equilibrium if the average distance between reactants B and C is correspondingly changed. In this way, the challenging task of separating time- and space-dependent parameters[60] has been simply evaded. Other theoretical predictions of the referred theory which we confirm include the zero-order dependence of K_A^{eq} on viscosity (Figure 2A). We have shown that the intermediate stage of the reaction of $^\bullet$NO and $O_2^{\bullet-}$ as studied by flash photolysis of ONOO$^-$ can be appropriately described in terms of mean field approximations (Supporting Information). The intermediate stage of diffusion-controlled reactions is frequently assumed to occur after the establishment of stationary concentration gradients and to obey the Smoluchowski steady-state equation (eq 15A and 15B). Given that some reported rate constants exceed this classical limit,[12,13] the steady-state Smoluchowski equation clearly fails. Moreover, the dependence of the observed rate

constant on temperature does not follow the trend exhibited by the Smoluchowski steady-state equation (Figure 3). Together, flash photolysis and equilibrium results suggest that the intermediate stage, even exponential, can be shown to reflect the diffusion control because systematic differences between observed rate constants that contradict the law of mass action should result if the distance between reactants is somehow varied.

D. Comments on the Observed Negative Activation Energy in the Reaction of $^\bullet$NO and $O_2^{\bullet-}$ at Equilibrium. A non-Arrhenius behavior with a negative value of activation energy ($E_a = -40 \pm 6$ kJ mol^{-1}) resulted from the experiments performed under equilibrium conditions and constant ONOO$^-$ concentration (Figure 3, thick line). This result may indicate that the reaction is thermally inactivated. Negative activation energies have found several explanations in the literature; if small, it has been taken as evidence of thermoneutrality (no thermal activation is needed). If the reaction can be kinetically decomposed in more than one step, the more common explanation for a significant negative activation energy requires that a rapid equilibrium should be followed by a low activation energy (or barrierless) step. In those scenarios, the higher the temperature, the faster the decomposition into reactants of the intermediate (which should be the reaction with the highest E_a of the three).[61,62] Notably, this has been proposed to be the case for the negative activation energy for a variety of radical reactions occurring in the gas phase,[63−67] including oxidation of $^\bullet$NO by dioxygen (O_2).[62,68] Negative activation energies have been also observed in some reactions in condensed organic phases.[69,70] Well-documented examples of negative activation energies for bimolecular reactions in aqueous media are scarce and mostly involve supercritical states.[71] The existence of an intermediate in the reaction between $^\bullet$NO and $O_2^{\bullet-}$ to yield ONOO$^-$ and its nature should be investigated, both by molecular dynamics simulations and experimentally. In our opinion, the existence of a covalent intermediate can be discarded. Formation of a contact pair in a solvent cage might be considered as requisite for the reaction to take place, and as starting point, the work by Simon and Tulub[48] shows that $^\bullet$NO$\cdots$O$_2^{\bullet-}$ complex can be modeled in the gas phase. Of notice, ZOOB theory makes no explicit statement about the apparent macroscopic activation parameters for forward bimolecular reaction rate constants. Nevertheless, the conclusion that the system is not in a thermodynamic equilibrium, in agreement with theory,[38,39] may also encourage new theoretical developments. Incomplete relaxation due to continuous correlated generation of highly reactive reactants has been suggested above to be a cause of ordering in the system at chemical equilibrium, in agreement with ZOOB theory.[36−39,54,56,57] An increased temperature might cause an increase in the anticorrelating effects of diffusion, increasing the fluctuation (noise) dependent relaxation rate, thus increasing the average distance between reactants. In fact, the range of forward rate constants values that we observe by changing the temperature (Figure 3, $7.0-40.0 \times 10^9$ M^{-1} s^{-1}) includes the range of values obtained by changing ONOO$^-$ concentration (Figure 4, $7.5-21.0 \times 10^9$ M^{-1} s^{-1}).

E. Final Comments. The present study hopefully contributes to the better understanding of the kinetics and thermodynamics of the diffusion-controlled reaction of $^\bullet$NO or $O_2^{\bullet-}$ to form ONOO$^-$. Two experimental limitations of this study are worth mentioning: one is to rely on a single technique for measuring $^\bullet$NO concentrations in equilibrium with ONOO$^-$, and the other is the lack of a direct evaluation of $O_2^{\bullet-}$ concentrations. It is hard to envision any alternative way of measuring $^\bullet$NO or $O_2^{\bullet-}$

with sufficient sensitivity and precision in the presence of a large excess of $ONOO^-$ at the highly alkaline conditions needed to stabilize $ONOO^-$. In other respects, additional information about this reaction−diffusion system will surely benefit from appropriate experiments under irreversible conditions with femto−picosecond UV and IR pulse pump−probe spectroscopy techniques.[72,73] Other likely informative experiments can result if chemically induced dynamic nuclear spin polarization (CIDNP) and photo-CIDNP methods[74,75] could be applied to the study of in-cage geminate radicals versus bulk radicals recombination problem in alkaline $ONOO^-$ samples.

The reaction type under study (A + B = C, with [A] = [B] and k_f diffusion controlled) has been extensively studied from the theoretical point of view. Overall, the uncovering of a distance-dependent reaction rate constant between $^\bullet NO$ or $O_2^{\bullet-}$ to form $ONOO^-$ at chemical equilibrium is to the best of our knowledge an unprecedented result in the experimental field of reversible diffusion-controlled reactions, which confirms some previous theoretical predictions for the behavior of reactions between ground-state reactants.[38−40] This confirmation about the macroscopic "final" state of a diffusion-controlled reversible reaction might find extensions into the kinetic theories of fast reversible diffusion-influenced reactions between excited reactants.[76] Our results indicate that the reported thermodynamic parameters for the reaction under consideration,[15−18,77−79] which assumed the validity of the law of mass action, should be revised and their distance/concentration dependence acknowledged. Regarding kinetic data, our results (Figure 4C, eq 21C) support diffusion-controlled distance-dependent forward rate constant for $ONOO^-$ formation $k_f^{310K} \geq 7.5 \times 10^9$ M^{-1} s^{-1} from $O_2^{\bullet-}$ and $^\bullet NO$ in dilute aqueous solution under equilibrium conditions.

Supporting Information Available: Data on the rate constant of peroxynitrite decay at pH >12, raw data on the effects of 50% glycerol on the concentration of $^\bullet NO$ in alkaline $ONOO^-$ solutions, and $ONOO^-$ formation time courses after flash photolysis of alkaline $ONOO^-$. This material is available free of charge via the Internet at http://pubs.acs.org.

References and Notes

(1) Pryor, W. A.; Squadrito, G. L. *Am. J. Physiol.* **1995**, *268*, L699.
(2) Pegel, K. H.; Laing, M. *S. Afr. J. Sci.* **2001**, *97*, 476.
(3) Ferrer-Sueta, G.; Radi, R. *ACS Chem. Biol.* **2009**, *4*, 161.
(4) Saran, M.; Michel, C.; Bors, W. *Free Radical Res. Commun.* **1990**, *10*, 221.
(5) Beckman, J. S.; Beckman, T. W.; Chen, J.; Marshall, P. A.; Freeman, B. A. *Proc. Natl. Acad. Sci. U.S.A.* **1990**, *87*, 1620.
(6) Radi, R.; Beckman, J. S.; Bush, K. M.; Freeman, B. A. *Arch. Biochem. Biophys.* **1991**, *288*, 481.
(7) Koppenol, W. H. *Redox Rep.* **2001**, *6*, 339.
(8) Pacher, P.; Beckman, J. S.; Liaudet, L. *Physiol. Rev.* **2007**, *87*, 315.
(9) Huie, R. E.; Padmaja, S. *Free Radical Res. Commun.* **1993**, *18*, 195.
(10) Kobayashi, K.; Miki, M.; Tagawa, S. *J. Chem. Soc., Dalton Trans.* **1995**, *17*, 2885.
(11) Goldstein, S.; Czapski, G. *Free Radical Biol. Med.* **1995**, *19*, 505.
(12) Kissner, R.; Nauser, T.; Bugnon, P.; Lye, P. G.; Koppenol, W. H. *Chem. Res. Toxicol.* **1997**, *10*, 1285.
(13) Nauser, T.; Koppenol, W. H. *J. Phys. Chem. A* **2002**, *106*, 4084.
(14) Kotomin, E.; Kuzovkov, V. V. *Modern Aspects of Diffusion-Controlled Reactions. Cooperative Phenomena in Bimolecular Processes*; Elsevier Science B. V.: Amsterdam, 1996; Vol. 34.
(15) Merényi, G.; Lind, J. *Chem. Res. Toxicol.* **1998**, *11*, 243.

(16) Goldstein, S.; Czapski, G.; Lind, J.; Merenyi, G. *Chem. Res. Toxicol.* **2001**, *14*, 657.
(17) Lymar, S. V.; Poskrebyshev, G. A. *J. Phys. Chem. A* **2003**, *107*, 7991.
(18) Sturzbecher, M.; Kissner, R.; Nauser, T.; Koppenol, W. H. *Inorg. Chem.* **2007**, *46*, 10655.
(19) Merenyi, G.; Lind, J. *Chem. Res. Toxicol.* **1998**, *11*, 243.
(20) Saha, A.; Goldstein, S.; Cabelli, D.; Czapski, G. *Free Radical Biol. Med.* **1998**, *24*, 653.
(21) Hughes, M. N.; Nicklin, H. G. *J. Chem. Soc. A* **1968**, 450–452.
(22) Bohle, D. S.; Glassbrenner, P. A.; Hansert, B. *Methods Enzymol.* **1996**, *269*, 302.
(23) Bohle, D. S.; Sagan, E. S. *Inorg. Synth.* **2004**, *34*, 36.
(24) Moller, M.; Botti, H.; Batthyany, C.; Rubbo, H.; Radi, R.; Denicola, A. *J. Biol. Chem.* **2005**, *280*, 8850.
(25) Fernandez-Ramos, A.; Miller, J. A.; Klippenstein, S. J.; Truhlar, D. G. *Chem. Rev.* **2006**, *106*, 4518.
(26) Ichino, T.; Fessenden, R. W. *J. Phys. Chem. A* **2007**, *111*, 2527.
(27) Lu, Y.; Lee, L.; Pan, J.; Xie, T.; Witek, H. A.; Lin, J. J. *J. Chem. Phys.* **2008**, *128*, 104317.
(28) Burshtein, A. I. *Adv. Chem. Phys.* **2009**, *2009*, 34.
(29) Atkins, P.; de Paula, J. *Atkin's Physical Chemistry*; Oxford University Press: New York, 2006; Vol. 1.
(30) Zacharia, I. G.; Deen, W. M. *Ann. Biomed. Eng.* **2005**, *33*, 214.
(31) Malinski, T.; Radomski, M. W.; Taha, Z.; Moncada, S. *Biochem. Biophys. Res. Commun.* **1993**, *194*, 960.
(32) Wise, D. L.; Houghton, G. *Chem. Eng. Sci.* **1968**, *23*, 1211.
(33) Lancaster, J. R., Jr. *Nitric Oxide* **1997**, *1*, 18.
(34) Kowert, B. A.; Dang, N. C. *J. Phys. Chem. A* **1999**, *103*, 779.
(35) Potter, M. J.; Luty, B. A.; Zhou, H. X.; McCammon, J. A. *J. Phys. Chem.* **1996**, *100*, 5149.
(36) Oshanin, G.; Burlatsky, S. *J. Phys. A* **1989**, *22*, L973.
(37) Oshanin, G. S.; Ovchinnikov, A. A.; Burlatsky, S. F. *J. Phys. A* **1989**, *22*, L977.
(38) Voituriez, R.; Moreau, M.; Oshanin, G. *J. Chem. Phys.* **2005**, *122*, 84103.
(39) Voituriez, R.; Moreau, M.; Oshanin, G. *Europhys. Lett.* **2005**, *69*, 177.
(40) Doktorov, A. B.; Kipriyanov, A. A. *J. Phys.: Condens. Matter* **2007**, *19*, 1.
(41) Goldstein, S.; Czapski, G.; Lind, J.; Merenyi, G. *Chem. Res. Toxicol.* **1999**, *12*, 132.
(42) Viggiano, A. A.; Midey, A. J.; Ehlerding, A. *Int. J. Mass Spectrom.* **2006**, *255*, 65.
(43) Goldstein, S.; Lind, J.; Merenyi, G. *Chem. Rev.* **2005**, *105*, 2457.
(44) Blough, N. V.; Zafiriou, O. C. *Inorg. Chem.* **1985**, *24*, 3502.
(45) Koppenol, W. H.; Moreno, J. J.; Pryor, W. A.; Ischiropoulos, H.; Beckman, J. S. *Chem. Res. Toxicol.* **1992**, *5*, 834.
(46) Bielski, B. H. J.; Cabelli, D. E.; Arudi, R. L. *J. Phys. Chem. Ref. Data* **1985**, *14*, 1041.
(47) Lim, C. H.; Dedon, P. C.; Deen, W. M. *Chem. Res. Toxicol.* **2008**, *21*, 2134.
(48) Simon, K.; Tulub, A. *Opt. Spectrosc.* **2009**, *107*, 46.
(49) Jursic, B.; Zdravkoski, Z. *Int. J. Quantum Chem.* **1995**, *54*, 161.
(50) East, A. *J. Chem. Phys.* **1998**, *109*, 2185.
(51) Scott, R. *Mol. Phys.* **1966**, *11*, 399.
(52) Scatchard, G.; Prentiss, S. S.; Jones, P. T. *J. Am. Chem. Soc.* **1932**, *54*, 2690.
(53) Lee, S.; Lee, J.; Shin, K. J. *Bull. Korean Chem. Soc.* **1994**, *15*, 311.
(54) Zel'Dovich, Y.; Ovchinnikov, A. *Sov. J. Exp. Theor. Phys. Lett.* **1977**, *26*, 440.
(55) Huppert, D.; Goldberg, S. Y.; Masad, A.; Agmon, N. *Phys. Rev. Lett.* **1992**, *68*, 3932.
(56) Burlatsky, S.; Oshanin, G.; Ovchinnikov, A. *Chem. Phys.* **1991**, *152*, 13.
(57) Gopich, I.; Ovchinnikov, A.; Szabo, A. *Phys. Rev. Lett.* **2001**, *86*, 922.
(58) Solntsev, K. M.; Huppert, D.; Agmon, N. *Phys. Rev. Lett.* **2001**, *86*, 3427.
(59) Agmon, N. *J. Phys. Chem. A* **2005**, *109*, 13.
(60) Agmon, N. *Chem. Phys. Lett.* **2006**, *417*, 530.
(61) Mozurkewich, M.; Benson, S. W. *J. Phys. Chem.* **1984**, *88*, 6429.
(62) Olson, L. P.; Kuwata, K. T.; Bartberger, M. D.; Houk, K. N. *J. Am. Chem. Soc.* **2002**, *124*, 9469.
(63) Menon, A.; Sathyamurthy, N. *J. Phys. Chem.* **1981**, *85*, 1021.
(64) Lii, R.; Gorse, R. A.; Sauer, M. C.; Gordon, S. *J. Phys. Chem.* **1979**, *83*, 1803.
(65) Chen, Y.; Rauk, A.; Tschuikow-Roux, E. *J. Phys. Chem.* **1991**, *95*, 9900.
(66) Mozurkewich, M.; Lamb, J. J.; Benson, S. W. *J. Phys. Chem.* **1984**, *88*, 6435.

Brownian Diffusion-Controlled Equilibria

J. Phys. Chem. B, Vol. 114, No. 49, 2010 **16593**

(67) Alvarez-Idaboy, J. R.; Mora-Diez, N.; Vivier-Bunge, A. *J. Am. Chem. Soc.* **2000**, *122*, 3715.

(68) Gadzhiev, O. B.; Ignatov, S. K.; Razuvaev, A. G.; Masunov, A. E. *J. Phys. Chem. A* **2009**, *113*, 9092.

(69) Shimomura, T.; Tölle, K. J.; Smid, J.; Szwarc, M. *J. Am. Chem. Soc.* **1967**, *89*, 796.

(70) Olson, J. B.; Koch, T. H. *J. Am. Chem. Soc.* **1986**, *108*, 756.

(71) Ghandi, K.; Addison-Jones, B.; Brodovitch, J.; McKenzie, I.; Percival, P. W.; Schüth, J. *Phys. Chem. Chem. Phys.* **2002**, *4*, 586.

(72) Oelkers, A. B.; Scatena, L. F.; Tyler, D. R. *J. Phys. Chem. A* **2007**, *111*, 5353.

(73) Banno, M.; Ohta, K.; Yamaguchi, S.; Hirai, S.; Tominaga, K. *Acc. Chem. Res.* **2009**, *42*, 1259.

(74) Closs, G.; Miller, R. J.; Redwine, O. D. *Acc. Chem. Res.* **1985**, *18*, 196.

(75) Goez, M.; Frisch, I. *J. Phys. Chem. A* **2002**, *106*, 8079.

(76) Popov, A. V.; Agmon, N.; Gopich, I. V.; Szabo, A. *J. Chem. Phys.* **2004**, *120*, 6111.

(77) Koppenol, W. H.; Kissner, R. *Chem. Res. Toxicol.* **1998**, *11*, 87.

(78) Merényi, G.; Lind, J.; Czapski, G.; Goldstein, S. *Inorg. Chem.* **2003**, *42*, 3796.

(79) Nauser, T.; Merkofer, M.; Kissner, R.; Koppenol, W. H. *Chem. Res. Toxicol.* **2001**, *14*, 348.